

EIGENVALUE ANALYSIS IN ELECTROMAGNETIC CAVITIES USING  
DIVERGENCE FREE FINITE ELEMENTS

Jian-She Wang and Nathan Ida

Department of Electrical Engineering  
The University of Akron  
Akron, OH 44325, U. S. A.

*Abstract* - The conventional node based finite element method frequently yields non-physical solutions to the vector eigenvalue problem in electromagnetic (EM) cavities. The non-physical modes are mainly due to inadequacy in enforcing the divergence free condition and boundary (as well as interface) conditions. The edge based finite element method with divergence free shape functions can delete spurious solutions due to these two reasons. This method has been used to solve various eigenvalue problems in both lossless and lossy cavities. No spurious modes are observed in the frequency range of interest. Good predictions to the lower modes are obtained in all examples. In addition to being a reliable tool for cavity mode analysis, the method also finds applications in characterization of materials when loaded in an EM cavity.

## INTRODUCTION

The finite element method provides a powerful tool for finding modes (especially the lower modes) in arbitrarily shaped, inhomogeneously loaded electromagnetic cavities [1,2,3]. Unfortunately, the standard finite element solution to the vector eigenvalue problem in a cavity consists of both physical and nonphysical modes. Among all the possible reasons responsible for the occurrence of spurious solutions, the following two are dominant. 1) Inadequacy in enforcing the divergence free condition, as a direct consequence of solving the *curlcurl* differential equation. 2) Inadequacy in enforcing the boundary and interface conditions since the direction for a nodal point can not be uniquely defined. There are many methods which can eliminate or reduce the nonphysical modes by enforcing the divergence free condition. Among them, the penalty method and the reduction method are commonly used ([4,5] and the references cited therein). This paper presents an alternate way, which, theoretically, can completely eliminate the nonphysical modes due to the mentioned two reasons. This is achieved by using finite "edge" elements having divergence free shape functions [6,7].

This paper is organized as follows. First, the basic formulations are introduced. Then, the divergence free, tetrahedral elements are used to discretize the formulations into algebraic eigensystems. These systems are arranged into various forms depending on the material properties and the solution method to be used. In order to show that the model is correct and free of spurious solutions, some typical examples, for which analytical or numerical solutions are available, are discussed. Finally, the present model is applied to material characterizations for microwave nondestructive testing purposes.

## BASIC FORMULATIONS

The problem under consideration is to find the resonant frequencies and the corresponding field distributions in a dielectric loaded EM cavity. The cavity wall,  $S$ , is assumed to be of arbitrary shape.

The interior of the cavity,  $\Omega$ , is characterized by  $(\mu_0\mu_r, \epsilon_0(\epsilon_r - j\epsilon_r'))(\vec{r}), \sigma(\vec{r}))$ , where  $\mu_0$  and  $\epsilon_0$  are the free space permeability and permittivity, respectively. The relative permeability and permittivity are assumed to be constant in each material. Since the cavity contains different materials;  $\vec{r}$  is used to denote the spatial dependence. With  $e^{j\omega t}$  variation implied, the modes in the cavity must be the solution of one of the following *curlcurl* equations:

$$\nabla \times \frac{1}{\mu_r} \nabla \times \vec{E} - k_0^2 \epsilon_r'(\vec{r}) \vec{E} = \vec{0}, \quad (1)$$

$$\nabla \times \frac{1}{\epsilon_r'(\vec{r})} \nabla \times \vec{H} - k_0^2 \mu_r \vec{H} = \vec{0}, \quad (2)$$

where  $L$  is a spatial scaling factor. The free-space wave number and the complex relative permittivity are given by

$$k_0 = L\omega\sqrt{\mu_0\epsilon_0}, \quad \epsilon_r' = \epsilon_r(1 - j \tan \delta). \quad (3)$$

The loss tangent is related to the imaginary part of the dielectric constant and conductivity of the material via

$$\tan \delta = \frac{\epsilon_r''}{\epsilon_r'} + \frac{\sigma\eta_0}{k_0\epsilon_r'}, \quad \eta_0 = \sqrt{\mu_0/\epsilon_0}. \quad (4)$$

At microwave frequencies, the first part is dominant. Typically,  $\epsilon_r$  is constant and  $\epsilon_r''$  increases with frequency. Throughout the paper,  $k_0$  (rads/m) is treated as the resonant frequency for numerical convenience. At material interfaces,  $\vec{E}$  and  $\vec{H}$  must be tangentially continuous.

To obtain numerical solutions to (1) and (2), it is advantageous to consider their weak forms: for the  $\vec{E}$  formulation,

$$\begin{aligned} \iint\int_{\Omega} \left( \frac{1}{\mu_r} \nabla \times \vec{E} \right) \cdot (\nabla \times \vec{w}_m) d\Omega - k_0^2 \iint\int_{\Omega} \epsilon_r'(\vec{r}) \vec{E} \cdot \vec{w}_m d\Omega \\ = jk_0\eta_0 \iint_S (\hat{n} \times \vec{H}) \cdot \vec{w}_m dS, \end{aligned} \quad (5)$$

and for the  $\vec{H}$  formulation,

$$\begin{aligned} \iint\int_{\Omega} \left( \frac{1}{\epsilon_r'(\vec{r})} \nabla \times \vec{H} \right) \cdot (\nabla \times \vec{w}_m) d\Omega - k_0^2 \iint\int_{\Omega} \mu_r \vec{H} \cdot \vec{w}_m d\Omega \\ = -\frac{jk_0}{\eta_0} \iint_S (\hat{n} \times \vec{E}) \cdot \vec{w}_m dS, \end{aligned} \quad (6)$$

where  $\vec{w}_m$  is any set of real vector weighting functions. By virtue of the weak forms, we can define, in the  $\vec{E}$  formulation, a homogeneous boundary condition  $\hat{n} \times \vec{E}$  (symmetry condition) and a natural boundary condition  $\hat{n} \times \vec{H}$ . Similarly in the  $\vec{H}$  case,  $\hat{n} \times \vec{H}$  is the homogeneous condition (symmetry condition), and  $\hat{n} \times \vec{E}$  is the natural condition. At microwave frequencies, it is quite accurate to assume that the tangential electric field vanishes on the cavity wall. If it is required to take into account the large but finite conductivity in the cavity wall, the following impedance boundary condition can be used [8]:

$$\hat{E} \times \vec{n} = Z_m \hat{n} \times (\hat{n} \times \vec{H}), \quad (7)$$

where  $Z_m = (1 + j)/\sigma\delta$ , is the surface impedance. The validity of (7) is limited in that the radii of curvature of the body must

be large with respect to the skin depth  $\delta_s$ . A modification can be made if necessary to avoid this limitation [8]. Since (5) and (6) are dual to each other, one needs to solve only one of them. However, they may yield eigenvalue systems of different types, depending on material properties. They also yield eigenvalue systems of different sizes, when boundary and symmetry conditions are imposed. Thus, one may choose  $\vec{E}$  or  $\vec{H}$  as the state variable according to particular problems.

The resonant frequency  $k_0$  and the corresponding eigenvector are, in general, complex, due to dielectric losses and cavity wall losses. It is necessary to operate in the complex domain. Only in the case where no loss is present, the resonant frequencies and eigenvectors are real, and the complex notation can be dropped.

### THE DIVERGENCE FREE FINITE ELEMENTS

To solve (6) in infinite dimensions is practically impossible. In this section, the finite element method is used to map the eigenproblem into finite dimensions. The standard (node based) finite element solution to the vector eigenvalue problem (2) contains nonphysical solutions in addition to true solutions. One obvious reason is that one is directly solving the *curlcurl* equation, leaving the divergence free condition,  $\nabla \cdot \vec{B} = 0$  or  $\nabla \cdot \vec{D} = 0$ , unspecified. In this work, we use the linear "edge" finite elements built on a tetrahedral model. The six vector shape functions in a tetrahedron element are

$$\vec{w}_n(\vec{r}) = \text{sgn}(n) \frac{l_n}{\delta} (\vec{p}_{7-n,1} \times \vec{p}_{7-n,2} + \vec{e}_{7-n} \times \vec{r}), \quad (8)$$

where  $n = 1, 2, \dots, 6$ , and other quantities are defined in [6]. These functions possess zero divergence. By introducing the following expansion in each element:

$$\vec{H}(\vec{r}) = \sum_{n=1}^6 H_n \vec{w}_n(\vec{r}), \quad \vec{E}(\vec{r}) = \sum_{n=1}^6 E_n \vec{w}_n(\vec{r}) \quad (9)$$

where  $H_n$  and  $E_n$  are the tangential components of  $\vec{H}$  and  $\vec{E}$  along edges, respectively,  $\vec{H}$  and  $\vec{E}$  are divergence free within the element. Thus, spurious modes for which  $\vec{H}$  and  $\vec{E}$  are not divergence free are deleted.

In the node based finite element method, it is necessary to define a nodal normal direction based on some sort of principle. With the tangential components used as unknowns in the "edge" based method, the nodal normal direction is no longer required. Since the expansions guarantee tangential continuities of field variables at the elemental interfaces, no special treatment is needed at material interfaces. Also, it is simple to impose boundary and symmetry conditions. For example, when it is required to compute a mode where the electrical field is symmetric to a plane, one can simply apply a natural condition  $\hat{n} \times \vec{H} = 0$  on the plane by setting the corresponding tangential unknowns on the plane to zero. Compared to the conventional method, the present analysis is simplified significantly.

One shortcoming of using FEM with linear basis functions like (8) to solve the vector eigenproblem, compared to the eigenfunction expansion type methods [9], is that the mode index information is lost. For a complicated geometric configuration, mode classification can be difficult, sometimes impossible. In practice, cavities and specimens may be manufactured and arranged in such a way, that the commonly used definitions for cavity modes (such as  $TE_{mnl}$ ,  $TM_{mnl}$ , Hybrid, etc.) are still applicable. Under these circumstances, the mode information may be retrieved by checking the eigenvectors.

### DISCRETIZED EIGENVALUE SYSTEMS

Assume that on  $S$ , the impedance condition (7) is satisfied. With the vector weighting functions chosen to be the same as the shape functions (8), (6) is reduced to a complex algebraic eigenvalue problem:

$$([A(k_0)] - k_0^2[B] + jk_0[G]) \{H\} = 0, \quad (10)$$

where the matrix coefficients are given by

$$a_{mn} = \iiint_{\Omega} \left( \frac{1}{\epsilon_r(1 - j \tan \delta)} \nabla \times \vec{w}_n \right) \cdot (\nabla \times \vec{w}_m) d\Omega, \quad (11)$$

$$b_{mn} = \iiint_{\Omega} \mu_r \vec{w}_n \cdot \vec{w}_m d\Omega, \quad (12)$$

$$g_{mn} = -\frac{Z_m}{\eta_0} \iint_S \hat{n} \times (\hat{n} \times \vec{w}_n) \cdot \vec{w}_m dS. \quad (13)$$

$[A(k_0)]$  denotes that matrix  $[A]$  depends on  $k_0$ , and it can be evaluated only when  $k_0$  is given, although  $[B]$  is a real constant matrix and  $[G]$  is a complex constant matrix.  $[G]$  is non-symmetric, and it has non-zero entries only on the boundary portion of the mesh. If there exists a symmetry plane (a magnetic wall),  $H_n$  along the corresponding edges on the plane equal to zero. These equations should be deleted from (10), otherwise erroneous modes may arise. The dependence of the loss tangent on frequency has made the solution of (10) more difficult as it can not be reduced to an algebraic eigenproblem. This means that standard eigen routines like those in "EISPACK" can not be utilized. However, one observes that (10) has a nonzero solution only if the determinant of the stiffness matrix is zero:

$$\det(R) = \det([A(k_0)] - k_0^2[B] + jk_0[G]) = 0. \quad (14)$$

Thus, the problem becomes one of searching for the zeros of (14) in the complex plane. Instead of directly computing the determinant of (14), one may check the singular values of  $[R]$ . Since  $[R]$  is a complex symmetric matrix, there exists a unitary matrix  $[U]$  such that  $[R]$  is diagonalized:  $[R] = [U][\Lambda][U]^T$ , where  $[\Lambda]$  is a real nonnegative diagonal matrix:  $[\Lambda] = \text{diag}(\lambda_1, \lambda_2, \dots, \lambda_N)$ . Then a zero of (14) must be at least a root of the following systems of equations of singular values [9]:

$$\lambda_i(k_0) = 0. \quad (15)$$

We mention that, since matrix  $[R]$  is fairly sparse, searching for its zeros or zero singular values may be very fast. In the case where the loss tangent does not vary with frequency (i.e., conductivity is zero and  $\epsilon_r$  is constant), (10) becomes a complex algebraic eigensystem. When no loss is present, a real, symmetric system is obtained.

In contrast to the  $\vec{H}$  formulation, the  $\vec{E}$  formulation gives an explicit expression. Let the imaginary part of the dielectric constant be a linear function of frequency:

$$\epsilon_r''(\vec{r}) = \epsilon_{ri}'' + k_0 K''(\vec{r}), \quad (16)$$

where  $\epsilon_{ri}''$  and  $K''$  are assumed to be positive constants. A third-order eigensystem is obtained:

$$([A] - k_0^2[B] + jk_0([C] + [G]) - jk_0^3[D]) \{E\} = 0, \quad (17)$$

where the coefficients in the real matrices are given by

$$a_{mn} = \iiint_{\Omega} \left( \frac{1}{\mu_r} \nabla \times \vec{w}_n \right) \cdot (\nabla \times \vec{w}_m) d\Omega, \quad (18)$$

$$b_{mn} = \iiint_{\Omega} (\epsilon_r - j\epsilon_{ri}'')(\vec{r}) \vec{w}_n \cdot \vec{w}_m d\Omega, \quad (19)$$

$$c_{mn} = \iiint_{\Omega} \eta_0 \sigma(\vec{r}) \vec{w}_n \cdot \vec{w}_m d\Omega, \quad (20)$$

$$d_{mn} = \iiint_{\Omega} K''(\vec{r}) \vec{w}_n \cdot \vec{w}_m d\Omega, \quad (21)$$

$$g_{mn} = -\frac{\eta_0}{Z_m} \iint_S \hat{n} \times (\hat{n} \times \vec{w}_n) \cdot \vec{w}_m dS. \quad (22)$$

Equation (17) may be rewritten as a complex, non-symmetric, generalized eigenvalue problem of  $k_0$ :

$$\begin{bmatrix} A & 0 & 0 \\ 0 & B & 0 \\ 0 & 0 & D \end{bmatrix} \begin{Bmatrix} E \\ \lambda E \\ \lambda^2 E \end{Bmatrix} = \lambda \begin{bmatrix} -C & -B & -D \\ B & 0 & 0 \\ 0 & D & 0 \end{bmatrix} \begin{Bmatrix} E \\ \lambda E \\ \lambda^2 E \end{Bmatrix}, \quad (23)$$

where  $\lambda = jk_0$ . When  $\epsilon''_{ri} = 0$  and the matrix  $[G]$  is dropped, equation (17) can be reduced to a real, non-symmetric eigensystem of triple size. In the case where  $K'' = 0$ , equation (23) can be reduced to either a real, non-symmetric eigensystem of double size:

$$\begin{bmatrix} A & 0 \\ 0 & B \end{bmatrix} \begin{Bmatrix} E \\ \lambda E \end{Bmatrix} = \lambda \begin{bmatrix} -C & -B \\ B & 0 \end{bmatrix} \begin{Bmatrix} E \\ \lambda E \end{Bmatrix}, \quad (24)$$

or a complex, symmetric system of double size:

$$\begin{bmatrix} A & 0 \\ 0 & B \end{bmatrix} \begin{Bmatrix} E \\ k_0 E \end{Bmatrix} = k_0 \begin{bmatrix} -jC & B \\ B & 0 \end{bmatrix} \begin{Bmatrix} E \\ k_0 E \end{Bmatrix}. \quad (25)$$

Finally, when no loss is present, a simple real, symmetric system is obtained:  $[A]\{E\} = k_0^2[B]\{E\}$ . In this work, real symmetric eigensystems are solved by Lanczos' method, non-symmetric systems by the QZ algorithm.

NUMERICAL RESULTS

To verify the method discussed above, consider first a spherical cavity (radius  $b$ ) concentrically loaded with a dielectric sphere (radius  $a = 0.1m$ ). Fig.1 shows the variation of the first four modes when the cavity radius  $b$  is varied. The two modes denoted by triangles and the two modes denoted by circles are obtained by different combinations of symmetry conditions. These curves are consistent with analytical solutions [10].

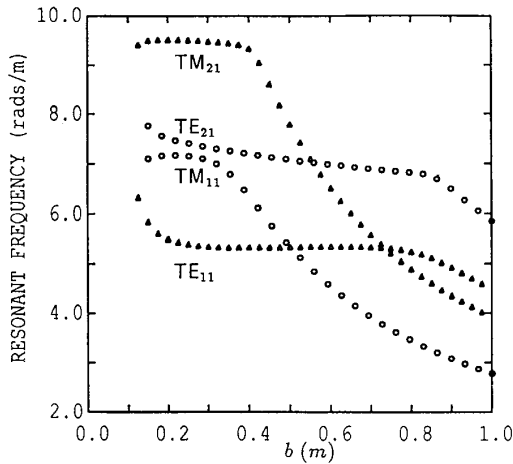


Fig.1 The first four modes of a dielectric sphere in a spherical cavity.

The following table shows the dominant mode in three empty cavities computed by the present model using different mesh sizes. It is found that a relatively small mesh size can yield good predictions to the lower frequencies, if the physical boundary of the cavity is

IEEE TRANSACTIONS ON MAGNETICS, VOL. 27, NO. 5, SEPTEMBER 1991 fitted well. For example, a better accuracy is obtained in the cube case than the other two cases. In addition, it seems that a lower error bound exists in the present model.

Cavity	Unknowns	Numer.	Anal.	Error
Cube (a=1m)	272	2.2301	2.221	+0.4%
	1840	2.2255	2.221	+0.2%
Cylinder (d=2m,r=.772m)	272	2.8952	2.855	+1.4%
	1840	2.8663	2.855	+0.4%
Sphere (r=1m)	90	2.8577	2.744	+4.1%
	272	2.8320	2.744	+3.2%
	1840	2.7704	2.744	+0.9%

The model is used next to characterize materials by the resonant frequencies of the loaded EM cavity. Some typical examples are given below, where the cavities are of simple shapes and isotropically loaded. Fig.2 shows the variation of the dominant mode with the size and the dielectric constant of the specimen, with a spherical specimen (radius  $a$ ) loaded in a cubic cavity (half side length  $b = 1.0m$ ). The family of curves correspond, vertically, to  $\epsilon_r = 1, 1.1, 1.5, 2, 3, 4, 8, 15, 36, 54, 72, 98$ , where the upper, horizontal line corresponds to  $\epsilon_r = 1$ .

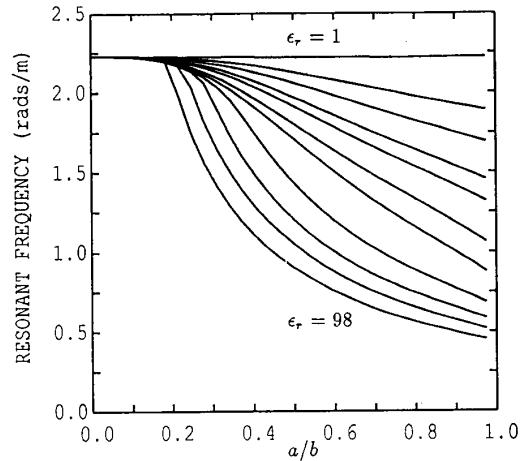


Fig.2 Dominant mode chart of a concentric sphere in a cubic cavity.

In Fig.3(a), a spheroid is loaded at the center of a cylindrical cavity, where the spheroid represents a soybean seed. The dielectric constant of the spheroid is assumed to be a linear function of water content  $c$ :  $\epsilon_r = 9 + (70 - j25) \cdot c$ . Fig.3(b) shows the variation of some modes with the water content. Obviously, by measuring the frequency shift, the water content of the soybean seed can be determined.

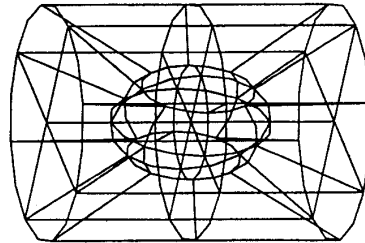


Fig.3(a) A lossy spheroid in a cylindrical cavity.

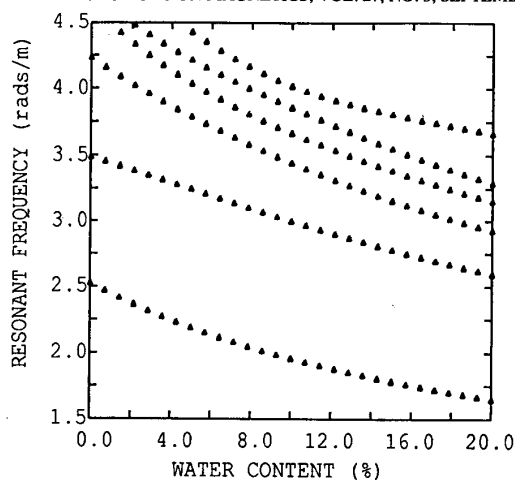


Fig.3(b) Mode chart of Fig.3(a).

Finally, consider a spherical specimen (radius=0.5m) loaded in a spherical cavity (radius=1.0m), where the loss tangent of the specimen depends on frequency. Fig.4 shows the variation of  $TM_{11}$  mode and  $TM_{21}$  mode with conductivity for  $\epsilon_r = 1, 2, 3, 4$ . Fig.5 shows the variation of some modes with  $K''$ , where the dielectric constant of the sphere is  $\epsilon_r = 36 - jK''k_0$ .

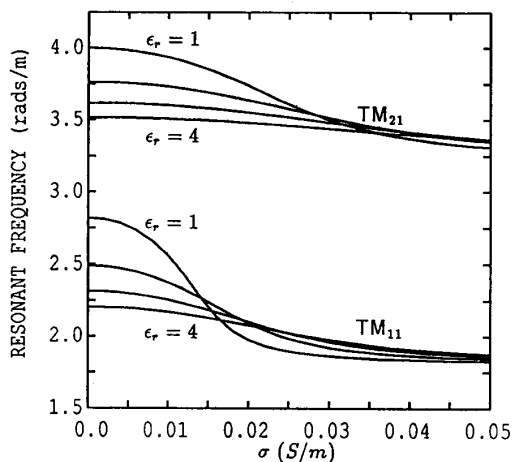


Fig.4 Mode chart of a lossy sphere in a spherical cavity: varying conductivity.

CONCLUSIONS

The "edge" based finite element method was used to compute the eigenmodes of inhomogeneously loaded electromagnetic cavities. No spurious modes were observed in the range of interest, as the divergence free condition was satisfied by the finite element shape functions. For the geometries discussed, the model can predict the lowest modes with satisfactory accuracy. The model was then applied to characterize lossy and lossless materials by the frequency shifts, for the materials in a cavity for non-destructive testing purposes. Future work will discuss the problem of a cavity loaded with lossy, anisotropic specimens.

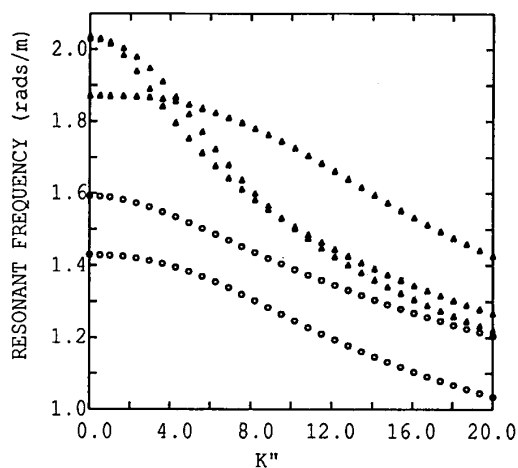


Fig.5 Mode chart of a lossy sphere in a spherical cavity: varying  $K''$ .

ACKNOWLEDGMENT

This work was supported in part by NSF Grant #EET8714628. Computational Resources on a CRAY Y-MP were provided by the Ohio Supercomputer Center. The "STLM" code used to solve real symmetric eigenvalue problems was provided by Thomas Ericsson, Department of Computer Science, Chalmers University of Technology, Sweden.

REFERENCES

- [1] J. B. Davies, F. A. Fernandez and G. Y. Philippou, "Finite Element Analysis of All Modes in Cavities with Circular Symmetry", IEEE Trans. Microwave Theory and Techniques, Vol. MTT-30, No.11, pp. 1975 - 1980, 1982.
- [2] M. Hara, T. Wada, T. Fukusawa and F. Kikuchi, "A Three Dimensional Analysis of RF Electromagnetic Fields by the Finite Element Method", IEEE Trans. Magnetics, Vol. MAG-19, No.6, pp. 2417 - 2420, 1983.
- [3] J. P. Webb, "The Finite-Element Method for Finding Modes of Dielectric-Loaded Cavities", IEEE Trans. Microwave Theory and Techniques, Vol. MTT-33, No.7, pp. 635 - 639, 1985.
- [4] J. P. Webb, "Efficient Generation of Divergence - Free Fields for the Finite Element Analysis of 3D Cavity Resonators", IEEE Trans. Magnetics, Vol. MAG-24, No.1, pp. 162 - 165, 1988.
- [5] A. Konrad, "A Method for Rendering 3D Finite Element Vector Field Solutions Non-Divergent", IEEE Trans. Magnetics, Vol. MAG-25, No.4, pp. 2822 - 2824, 1989.
- [6] M. L. Barton and Z. J. Cendes, "New Vector Finite Elements for Three-Dimensional Magnetic Field Computation", J. Appl. Phys., Vol.61, No.8, pp. 3919 - 3921, 1987.
- [7] K. Sakiyama, H. Kotera, A. Ahagon, "3-D Electromagnetic Field Mode Analysis Using Finite element Method by Edge Element", IEEE Trans. Magnetics, Vol.26, No.5, pp. 1759 - 1761, 1990.
- [8] R. Mittra (ed.), Computer Techniques for Electromagnetics, Pergamon, Press, pp.172-173, 1973.
- [9] Wenxin Zheng, "Direct and Inverse Resonance Problems for Shielded Composite Objects Treated by Means of the Null-Field Method", IEEE Trans. Antennas Propagat., Vol.37, No.11, pp. 1732 - 1739, 1989.
- [10] D. Kajfez and P. Guillon (eds), Dielectric Resonators, Artech House Inc., p.403, 1986.